mg, 15.9 mmol) in dry THF (3.0 mL) at -78 °C. After being stirred for 20 min at -78 °C, the mixture was allowed to warm to 0 °C and worked up as usual to give a colorless oil (96 mg, 64%), which solidified on trituration with petroleum ether. Recrystallization from petroleum ether gave colorless needles: mp 41-42 °C; IR (KBr) 3070-2950, 1740, 1600, 1535, 1430, 1320, 1160 cm^{-1}; ^1H NMR ($CDCl_3$) δ 0.14 (d, J = 3.5 Hz, H-10-anti), 1.43 (d, J = 3.5 Hz, J(10-syn,9) = 0.5 Hz, H-10-syn), 3.64 (s, Me), 3.67 (dd, J = 2.0 and 2.0 Hz, H-9), 5.25 (dd, J = 2.0 and 6.0 Hz, H-8), 6.24 (dd, J = 2.0 and 6.0 Hz, H-7), 5.74-5.88 (m, H-3,4), 6.10-6.30 (m, H-2,5). Anal. ($C_{12}H_{12}O_2$) C, H.

Diels-Alder reaction of 13 with isobenzofuran was carried out in the same manner as described for the formation of **4** from **1** to produce a mixture of **17** and **16**, which was separated by preparative TLC using 1:1 hexane-ether elution. **16**: colorless needles (8%); mp 82-83 °C; IR (KBr) 3040-2950, 1730, 1455, 1435, 1340, 1270-1150, 970 cm^{-1}; ^1H NMR, see Table I. Anal. ($C_{20}H_{18}O_3$) C, H. **17**: colorless needles (10%); mp 85-86 °C; IR (KBr) 3050-2960, 1733, 1460, 1435, 1260-1145 cm^{-1}; ^1H NMR (see Table I). Anal. ($C_{20}H_{18}O_3$) C, H.

Diels-Alder reaction of 11 with isobenzofuran was carried out in a similar manner to that described above to give **24**: colorless needles (9.0%); mp 86-87 °C; IR (KBr) 3040-2929, 1460, 1350, 1240, 970, 865, 830 cm^{-1}; ^1H NMR, see Table I; mass spectrum, m/e (%) 320 (3), 215 (14), 202 (57), 129 (32), 128 (68), 118 (66), 73 (100).

Reduction of 13. According to the usual procedure, **13** (150 mg) was treated with LAH (45.4 mg, 1.19 mmol) in dry ether (10 mL) at 0 °C for 1 h to give **18**: colorless oil; 136 mg (100%); IR (neat) 3350, 3060-2870, 1598, 1535, 1333, 1060, 1015, 978, 750 cm^{-1}; ^1H NMR ($CDCl_3$) δ -0.07 (d, J = 3.5 Hz, H-10-anti), 1.60 (d, J = 3.5 Hz, H-10-syn), 2.05 (br s, OH), 3.13 (ddt, H-9), 3.82 (m, CH_2O), 5.23 (dd, J = 6.0 and 2.0 Hz, H-8), 5.78-6.50 (m, H-7,2,3,4,5); mass spectrum, m/e (%) 160 (15), 129 (63), 128 (100).

Derivation of 18 to 10. To a stirred solution of **18** (32 mg, 0.2 mmol) in methylene chloride (4.0 mL) was added boron trifluoride etherate (7.6 μL) at 0 °C; then ethereal diazomethane solution (2.0 mL) was added dropwise. After the solution stirred at 0 °C for 1 h, the precipitate which formed was filtered off and the filtrate was poured into ice water. Extraction with methylene chloride, washing the extract with aqueous $NaHCO_3$, drying (Na_2SO_4), and solvent evaporation left a colorless oil (20 mg, 57%), which was chromatographed on silica gel. The product obtained had spectral data identical with those of **10**.

Derivation of 18 to 7 via 19. A mixture of **18** (148 mg, 1 mmol), pyridine (118.65 mg, 1.5 mmol), tosyl chloride (285.9 mg, 1.5 mmol), and methylene chloride (8 mL) was heated at reflux for 19 h. To this was added again a mixture of tosyl chloride (0.5 mmol) and pyridine (0.5 mmol), and heating was further continued for 12 h at reflux. The reaction mixture was cooled, diluted with water, neutralized with 2 N HCl, and extracted with ether. Ether extracts were washed with aqueous $NaHCO_3$ and dried. Removal of the solvent gave **19** as a colorless oil; 258 mg (85%). A solution of this oil (0.85 mmol) in ether (8 mL) was heated at reflux with LAH (32.26 mg, 0.85 mmol) for 13 h. After the solution cooled to room temperature, excess hydride was destroyed with water and the ether layer was dried (Na_2SO_4). Removal of the solvent and column chromatography of the oily residue gave a colorless oil (75 mg, 61%), which had spectral data identical with those of **7**. **19**: ^1H NMR ($CDCl_3$) δ -0.25 (d, J = 3.5 Hz, H-10-anti), 1.30 (d, J = 3.5 Hz, H-10-syn), 2.45 (s, Me), 3.23 (ddt, J = 7.5, 2.0 and 2.0 Hz, H-9), 4.12 (d, J = 7.5 Hz, CH_2O), 5.05 (dd, J = 6.0 and 2.0 Hz, H-8), 5.65-6.35 (m, H-2,3,4,5,7), 7.33 and 7.85 (two AB-type d's, J = 8.0 Hz, Ph).

Reduction of 15 was carried out in the same way as described for the reduction of **13**. **20**: colorless oil (73%); IR (neat) 3350, 3040-2870, 1600, 1535, 1330, 1065, 1020, 970, 750 cm^{-1}; ^1H NMR ($DCCl_3$) δ 0.05 (d, J = 3.5 Hz, H-10-anti), 1.47 (d, H-10-syn), 1.83 (br s, OH), 2.97 (m, H-9), 3.57 (m, CH_2O), 5.20 (dd, J = 6.0 and 2.0 Hz, H-8), 5.70-6.68 (m, H-7,2,3,4,5); mass spectrum, m/e (%) 160 (20), 142 (35), 141 (32), 129 (75), 128 (100), 127 (55), 115 (30), 102 (25).

9-*endo*-Methoxymethyltricyclo[4.3.1.0]decatriene (22). The endo alcohol **20** was methylated by the same method as the formation of **10** from **18** to give **22**: colorless oil (46%); ^1H NMR ($CDCl_3$) δ 0.00 (d, J = 3.0 Hz, H-10-anti), 1.47 (d, J = 3.0 Hz, H-10-syn), 2.97-3.75 (m, H-9 and CH_2O), 3.33 (s, Me), 5.15 (dd, J = 6.0 and 2.0 Hz, H-8), 6.10 (br d, J = 6.0 Hz, H-7), 5.75-6.55 (m, H-2,3,4,5).

9-*endo*-Tosyloxymethyltricyclo[4.3.1.0]decatriene (21) was prepared by the same method as described for the preparation of **19**. **21**: colorless oil (88%); ^1H NMR ($CDCl_3$) δ 0.03 (d, J = 3.0 Hz, H-10-anti), 1.42 (d, H-10-syn), 2.50 (s, Me), 3.10 (m, H-9), 3.51-4.21 (m, CH_2O), 5.08 (dd, J = 6.0 and 2.0 Hz, H-8), 5.70-6.75 (m, H-2,3,4,5,7), 7.10 and 7.87 (two AB-type d's, J = 8.0 Hz, Ph).

9-*endo*-Methyltricyclo[4.3.1.0]decatriene (23) was prepared from **21** by the same method as described for the derivation of **7** from **19**. **23**: colorless oil (61%); ^1H NMR ($CDCl_3$) δ 0.00 (d, J = 3.0 Hz, H-10-anti), 0.93 (d, J = 7.0 Hz, Me), 1.53 (d, J = 3.0 Hz, H-10-syn), 2.88 (ddq, J = 2.0, 2.0, and 7.0 Hz, H-9), 5.27 (dd, J = 6.0 and 2.0 Hz, H-8), 5.68-6.58 (m, H-7,2,3,4,5).

Acknowledgment. We thank Dr. H. Fujimoto of Kyoto University and Dr. S. Inagaki of Gifu University for drawing contour maps and helpful discussion about the orbital interactions. We also acknowledge Dr. Y. Fukazawa and Professor S. Ito of Tohoku University for their help in using the MMI program.

Long-Range Triplet-Triplet Energy Transfer within Metal-Substituted Hemoglobins

Haya Zemel and Brian M. Hoffman*

Contribution from the Department of Chemistry, Northwestern University, Evanston, Illinois 60201. *Received June 27, 1980*

Abstract: We present a detailed analysis of the long-range (Förster-type) triplet-to-triplet energy transfer between the photoexcited triplet states of the zinc and magnesium protoporphyrin IX chromophores of Zn- and Mg-substituted hemoglobin. The observations of this rarely detected process are made in fluid solution and at ambient temperature by monitoring the time dependence of triplet-triplet absorption subsequent to flash excitation. This appears to be the first time that rate constants have been measured for Förster energy transfer (triplet) between chromophores at crystallographically known distances and orientations. To provide further reference data on chromophore-protein complexes, we have measured the triplet decay rates for zinc myoglobin (k_1 = 70 ± 5 s^{-1}) and magnesium myoglobin (k_1 = 24 ± 1 s^{-1}) and the bimolecular rate constant for quenching the zinc myoglobin triplet by O_2 (k_q = 1.25 × 10^8 m^{-1} s^{-1}) and by dithionite (k_q = 2.4 × 10^6 m^{-1} s^{-1}).

Introduction

Since its elucidation by Förster, about 30 years ago,[1] long-range (dipole-dipole) electronic energy transfer has been extensively studied and widely used in the investigation of photoreactions and the characterization of molecules in their excited state.[2] This energy-transfer process is extremely sensitive to interchromophoric distances, and singlet-energy donors are routinely used to estimate both intra- and intermolecular distances in protein systems. Energy-transfer reactions involving triplet donors can occur by

(1) Förster, T. *Ann. Phys. (Leipzig)* **1948**, *2*, 55.

(2) (a) Turro, N. J. "Modern Molecular Photochemistry"; The Benjamin/Cummings Publishing Co.: Menlo Park, Calif., 1978. (b) Chapter 2 of "Energy Transfer and Organic Photochemistry"; Lamola, A. A., Turro, N. J., Eds.; Interscience Publishers, New York, 1969.

0002-7863/81/1503-1192$01.25/0

Table I

donor transition	acceptor transition	mechanism
(1) $T_1 \rightarrow S_0$	$S_0 \rightarrow T_1$	exchange
(2) $T_1 \rightarrow S_0$	$T_1 \rightarrow S_1$	exchange
(3) $T_1 \rightarrow S_0$	$S_0 \rightarrow S_1$	dipole-dipole
(4) $T_1 \rightarrow S_0$	$T_1 \rightarrow T_2$	dipole-dipole

several mechanisms (Table I), but almost invariably they proceed via a short-range exchange process. Such reactions involve collisions between chromophores and include the so-called "triplet–triplet" transfer and triplet–triplet (T–T)[3] annihilation processes described in Table I, lines 1 and 2, respectively.

Förster-type transfer of triplet excitation energy is a rare phenomenon and is not well documented. There have been very few observations of triplet–singlet transfer (line 3, Table I)[4] and only a single report of the annihilation resulting from long-range T–T transfer between excited triplets (line 4, Table I).[5] The two types of long-range triplet-energy transfer have been detected only in solid matrices in which the chromophores are rigidly held at distances larger than needed for the exchange mechanism. Considering reaction 4, long-range T–T annihilation, although the phenomenon was convincingly demonstrated, an accurate comparison between experiment and theory was impossible because the annihilation process itself led to an astatistical distribution of triplets in the polymer matrix, thus invalidating theoretical models.[5] We here present measurements of long-range triplet–triplet annihilation which are amenable to detailed theoretical analysis and which involve chromophores at known distances and in known relative orientations. Indeed, to the best of our knowledge this work represents the first detailed study of *any* long-range energy-transfer process in which interchromophoric distances *and* orientations both are rigorously known.

In the course of our studies of metal-substituted hemeproteins,[6] we have been examining hemoglobins in which the four hemes have been replaced by a closed-shell metalloporphyrin, in particular employing the divalent zinc[7] and magnesium[8] metallomacrocycles. In this report we demonstrate that such proteins provide an ideal system for the observation and characterization of long-range intramolecular triplet–triplet energy transfer in fluid solution at room temperature. The several features which uniquely suit the MHb for such studies have been most fully exploited with ZnHb and include the following: (1) excitation of the metalloporphyrin into its lowest triplet state is achieved with a high quantum yield; (2) the intrinsic lifetime of the triplet excited state is long; (3) the porphyrins are held in fixed positions with interchromophore distances and orientations fully known from X-ray diffraction studies.[9]

A second and distinct attribute of this experimental system lies in its utility as a model for components of the photosynthetic apparatus. There is considerable evidence that in vivo chlorophyll typically occurs in a well-defined complex with protein.[10] Zinc- and magnesium-substituted hemoglobins provide an excellent, well-defined, model system for studying the excitation energy transfer and electron-transport reactions within and between such chlorophyll–protein complexes.

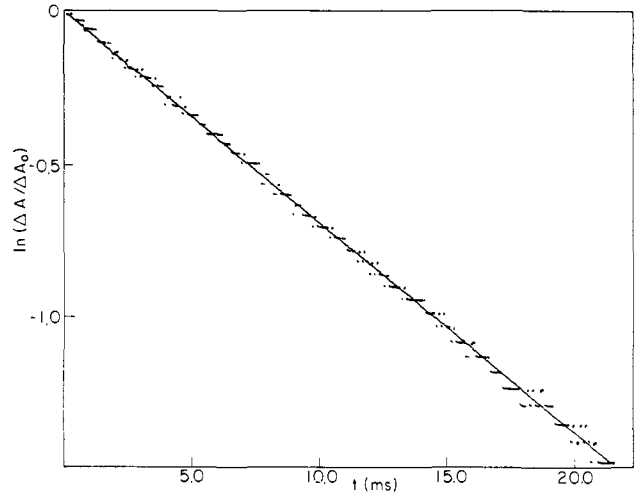

Figure 1. A typical plot of ZnMb triplet decay monitored at 427.5 nm in fully deoxygenated 0.1 M KPi buffer (pH 7.0) at room temperature.

Experimental

Zinc and magnesium were inserted into protoporphyrin (Sigma) by literature methods.[11] Sperm whale myoglobin was obtained from Sigma and was purified by the method of Brown.[12] Human hemoglobin A was prepared from fresh pooled blood and zinc- and magnesium-substituted hemoglobin and myoglobin were prepared by our published procedures.[13] The protein monomer concentrations for ZnHb were obtained from the Soret maximum extinction coefficient: ϵ_{max}(ZnHb) = 122 mM^{-1} cm^{-1}.[14] Concentrations for ZnMb, MgHb, and MgMb were only estimated, by assuming the same extinction at the respective Soret maxima. Samples for flash photolysis were prepared in the following way: aqueous potassium phosphate buffer (0.1 M) was first extensively deoxygenated in a tonometer by repeatedly evacuating and refilling with N_2. Concentrated protein which had been separately flushed with N_2 was then added anaerobically to the tonometer by using an airtight syringe. Solutions of triplet quenchers were completely deaerated in Schlenk-ware before addition to the tonometer by airtight syringe. Oxygen titrations were carried out by adding aliquots of air to the evacuated tonometer. Unless otherwise stated, measurements were performed in pH 7.0 buffer at room temperature, 22 ± 2 °C.

The minicomputer-interfaced flash photolysis apparatus, employing either an RCA 1P28 or 4840 detector, is described elsewhere.[15] Early measurements employed a Xenon Corp. Model No. 457 flash lamp as the excitation source. The need for better time resolution led to the incorporation of an ElectroPhotonics Model 33 dye laser. The laser was untuned and the dye used was Rhodamine 6G (emission maximum at 590 nm). Kinetic progress curves could be computer-fitted by a nonlinear regression routine which employed the algorithm of Marquardt.[16]

Results

(I) ZnHb and ZnMb Spectra. Flash illumination of either ZnMb or ZnHb yields a transient absorbance change with a rise which follows the flash profile (≤20 μs) and a decay which is observable on a millisecond time scale (Figure 1). The process is fully reversible, with complete recovery of the starting material after each flash. Figure 2 presents absorbance spectra of ZnMb and ZnHb and the wavelength-dependent change in absorption, ΔA_0, produced by a flash of uniform intensity. Although the decay kinetics of ZnMb are simple, those of ZnHb are not (see below). As a result, for both proteins, the value of ΔA_0 at each wavelength was obtained by fitting the initial 5–10% of the decay to the

(3) Abbreviations used: T–T = triplet–triplet; MHb and MMb = metal (M)-substituted hemoglobin and myoglobin; MProtoPor and MUrPor = metalloprotoporphyrin IX and uroporphyrin.

(4) Ermolaev, V. L.; Sveshnikova, E. B. *Acad. Nauk USSR, Acad. Sci. Bull. Phys.* **1962**, *26*, 29. Bennett, R. G.; Schwenker, R. P.; Kellogg, R. E. *J. Chem. Phys.* **1964**, *41*, 3040.

(5) Kellogg, R. E. *J. Chem. Phys.* **1964**, *41*, 3046–3047.

(6) Hoffman, B. M. In "The Porphyrins", Dolphin, D. Ed.; Academic Press: New York, 1979, Vol. VII, pp 403–444.

(7) Hoffman, B. M. *J. Am. Chem. Soc.* **1975**, *97*, 1688–1694.

(8) To be submitted for publication.

(9) (a) Ten Eyck, L. F.; Arnone, A. *J. Mol. Biol.* **1976**, *100*, 3–11. (b) Fermi, G. *Ibid.* **1975**, *97*, 256.

(10) See: (a) Matthews, B. W.; Fenna, R. E.; Bolognesi, M. C.; Schmid, M. F.; Olson, J. M. *J. Mol. Biol.* **1979**, *131*, 259–285; (b) Loach, P. A. In "Progress in Bioorganic Chemistry", Kaiser, E. T., Kezdy, F. J. Eds.; Wiley-Interscience: New York, 1976; Vol. 4, pp 89–192.

(11) Adler, A. D.; Longo, F. R.; Kampas, F.; Kim, J. *J. Inorg. Nucl. Chem.* **1970**, *32*, 2443.

(12) Brown, W. D. *J. Biol. Chem.* **1961**, *236*, 2238–2240.

(13) Scholler, D. M.; Wang, M.-Y. R.; Hoffman, B. M. In "Methods in Enzymology"; Fleischer, S., Packer, L. Eds.; Academic Press: New York, 1978; Vol. III, Part C, pp 487–493.

(14) Leonard, J. J.; Yonetani, T.; Callis, J. B. *Biochemistry* **1974**, *13*, 1460–1464.

(15) Stanford, M. A.; Swartz, J. C.; Phillips, T. E.; Hoffman, B. M. *J. Am. Chem. Soc.* **1980**, *102*, 4492–4499.

(16) Bevington, P. R. "Data Reduction and Error Analysis for the Physical Sciences", McGraw-Hill: New York, 1969.

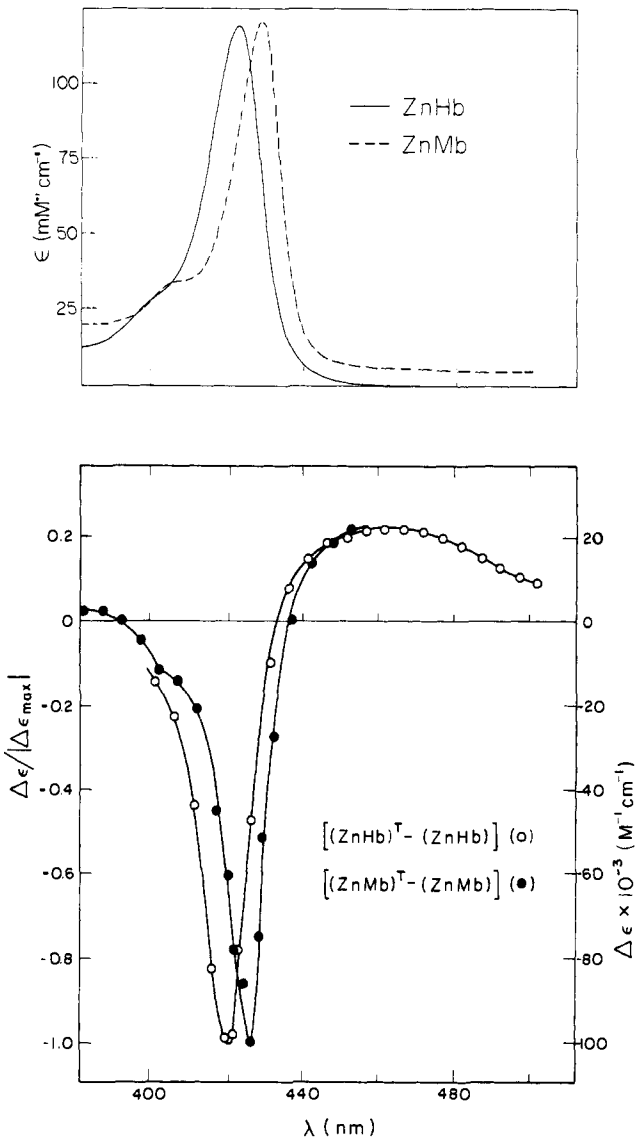

Figure 2. Soret-region spectra of ZnHb and ZnHb: upper trace, absorption spectra of ground-state ZnHb and ZnMb; lower trace, {[triplet] - [ground]} difference spectra for ZnHb and ZnHb. The right-hand ordinate is calculated as described in the text.

equation $\Delta A_t = \Delta A_0 e^{-kt}$ by least-squares regression. These spectra have as their most pronounced characteristic a strong negative feature with its minimum slightly to the red (0.5–1.0 nM) of the ground-state Soret peak. In addition, they show a broad and relatively weak absorbance increase at longer wavelength and with a maximum absorbance (not shown) in the red, at ~750 nm. In combination with the kinetic behavior, these several features of the kinetic difference spectrum identify the transient as the lowest excited triplet state of ZnProtoPor.[17,18]

Laser excitation is capable of producing essentially 100% triplet formation, as indicated by a saturation of ΔA_0 with increasing light intensity; by comparison, the xenon flash tube is capable of generating ~60% triplets. The achievement of complete population inversion is presumably possible because of multiple excitations during the relatively long pulses (~0.8 μs, laser, ~20 μs, flash) and permits us to calculate the values for $\Delta\epsilon = \epsilon$(ground) $- \epsilon$(triplet) and ϵ_{max}(triplet). In the case of ZnHb this was done by using $\epsilon_{421} = 122$ mM^{-1} cm^{-1} for the ground-state Soret maximum.[14] The resulting $\Delta\epsilon$ are given in Figure 2. The extinction coefficient for the ZnHb triplet Soret maximum (~422 nm) is 24 ± 5 mM^{-1} cm^{-1}, and it is practically identical with the value reported for the ZnUrPor triplet.[18] The extinction values for ZnMb triplet are roughly the same as those for ZnHb but could not be determined because the ground-state ϵ_{max} is not accurately known.

(II) Triplet Decay Kinetics. (A) ZnMb. (a) Decay in the Absence of Quenchers. The disappearance of the ZnMb triplet in rigorously oxygen free solution obeys first-order kinetics for more than 80% of the decay process. A typical plot of log ΔA vs. t is shown in Figure 1. A rate constant of 70 ± 5 s^{-1} was obtained from a linear least mean squares fit to the data. Results presented below confirm that this value is not artificially increased because of triplet quenching by residual O_2. All rate measurements were performed at 427.5 nm where the difference spectrum peaks. Small variations of the apparent triplet decay rate with wavelength have been observed (±15%) and can be correlated with the presence of another transient with a rise time similar to that of the triplet decay and a much slower disappearance rate. This transient was followed separately at the ZnMb triplet-ground isosbestic point, 437 nm, where its maximal ΔA was positive and 100 times smaller than $|\Delta A_0|$ at 427.5 nm. The exact contribution of this transient at 427.5 nm could not be determined; however, the absence of a distinguishable slow component suggests that the effect there is negligible. No positive identification of this transient has been made so far. Reversible photoreduction or photooxidation of the triplet[18] is the most plausible explanation, but a minor impurity species is also possible.

The decay of the photoexcited ZnMb triplet is independent of the ZnMb concentration and of the fractional population of the triplet state. In particular, no evidence of second-order contributions is detected in samples containing an initial triplet concentration of from 10 to 20 μM. This finding allows us to set an upper limit to the ZnMb second-order, intermolecular triplet–triplet (T–T) annihilation rate constant of less than approximately 10^6 M^{-1} s^{-1}, a value more than 3 orders of magnitude lower than the triplet–triplet decay constant reported for solution zinc tetraphenylporphine.[17] The absence of an observable bimolecular T–T annihilation process with ZnMb is presumably due to shielding of the porphyrin by the protein, which prevents a direct encounter between triplets and thus decreases the rate of energy transfer compared to that of the free zinc porphyrin in solution.

The value of 70 ± 5 s^{-1} for the ZnMb triplet decay rate constant is similar to that reported for zinc tetraphenylporphine[17] and lower than the value of ~250 s^{-1} found for zinc uroporphyrin.[18] However, unlike the previous values, the rate constants reported here are measured directly rather than estimated from the intercept in quenching experiments and are therefore much more accurate.

(b) Decay in the Presence of Quenchers. Addition of O_2 to ZnMb solutions decreases the lifetime of the ZnMb triplet. However, O_2 not only quenches the triplet but also reacts chemically with the excited ZnMb. Upon repeated photolysis of ZnMb in the presence of O_2, the triplet state lifetime lengthens, indicating a loss of O_2, and the Soret band absorption decreases, indicating destruction of the porphyrin chromophore and/or protein denaturation and precipitation. If there is only a trace of oxygen present, the triplet decay rate constant eventually reaches a final value of 70 s^{-1} and the Soret absorption becomes stable as well. These observations suggest that after a sufficient number of flashes all O_2 is consumed. The most probable direct product of the quenching process is singlet oxygen, which is well-known to react readily with porphyrins;[19] both free zinc porphyrins and ZnMb or ZnHb are destroyed slowly if kept in light under air but are stable to light if O_2 is replaced by N_2. This photosensitivity provided a means of assuring that a sample had been totally deoxygenated, for only then was the absorption spectrum stable to photolysis. In the event that a minor trace of oxygen remained, it was consumed in a few flashes without significant harm to the sample.

(17) (a) Pekkarinen, L.; Linschitz, H. *J. Am. Chem. Soc.* **1960**, *82*, 2407–2411. (b) Linschitz, H.; Steel, C.; Bell, J. A. *J. Phys. Chem.* **1962**, *66*, 2574–2576.

(18) Carapellucci, P. A.; Mauzerall, D. *Ann. N.Y. Acad. Sci.* **1975**, *244*, 214–238.

(19) See for example: Wasser, R. K. W.; Fuhrop, J.-H. *Ann. N.Y. Acad. Sci.* **1973**, *206*, 533–548.

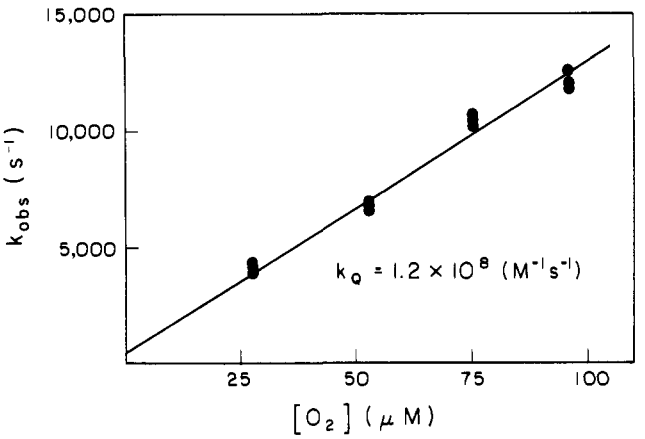

Figure 3. Oxygen dependence of the observed ZnMb triplet decay rate, assuming $[O_2] = (1.38 \text{ mM atm}^{-1}) \times P_{O_2}$.

The oxygen reaction made it difficult to determine the quenching rate constants by means of an oxygen titration because the O_2 concentration changed with each flash. We overcame this obstacle by (1) using the highest oxygen concentrations consistent with a triplet decay rate which could be accurately measured, thus decreasing the percentage of $[O_2]$ variation and (2) reequilibrating the solution with the oxygen atmosphere in the tonometer prior to each flash excitation. The amount of porphyrin destruction per flash was so small that it did not influence the rate determinations. Figure 3 shows a plot of the observed first-order decay rate constant (k_{obs}) vs. $[O_2]$. A second-order rate constant of 1.25×10^8 M^{-1} s^{-1} for quenching of ZnMb triplet by oxygen was obtained from the data by a least-squares fit. This value is in excellent agreement with values previously reported for the metal-free protoporphyrin-substituted hemoglobin[20] and myoglobin.[21]

Sodium dithionite ($Na_2S_2O_4$) is routinely used to remove traces of oxygen from deaerated heme-protein samples. However, it could not be used in the study, since we observed that the ZnMb triplet decay was accelerated in the presence of dithionite. The decay progress curves could not be satisfactorily fitted by pure first-order kinetics but were well described by a scheme in which a major component (85–90%) decayed with a rate linearly dependent on dithionite concentration and a minor component exhibited a dithionite-independent rate, $k = 75 \pm 10$ s^{-1}. The latter component presumably reflects a minority form of the protein and is not considered further. The first-order rate of the major component obeyed the simple quenching equation, $k_{obs} = k_0 + k_q[Q]$. The second-order rate constant for the quenching of ZnMb triplet by dithionite is $k_q = 2.4 \times 10^6$ M^{-1} s^{-1}, and the dithionite-free triplet decay rate obtained from the intercept is $k_0 = 69 \pm 15$ s^{-1}. The latter equals the directly measured rate of 70 ± 5 s^{-1}.

The dithionite quenching rate is rather low and the quenching mechanism unclear. In order to examine the possibility of a "heavy-atom" effect due to the sulfur, we followed the ZnMb triplet decay in the presence of $Na_2S_2O_6$. Absolutely no quenching was observed up to 1 mM of $Na_2S_2O_6$ although the effect of dithionite was detectable at 0.04 mM. In fact, even potassium iodide, which is more likely to exert a heavy-atom effect, showed no quenching of the ZnMb triplet up to 1 M concentration. It seems plausible to suggest that a rapid, reversible, electron-transfer process occurs, although no direct evidence was obtained for this. However, a possibly related phenomenon is the appearance of a small peak (465 nm) in the ground-state absorption spectrum after many flashes in the presence of dithionite. This peak disappeared slowly but completely when the sample was exposed to air, suggesting that it was due to a reduced species which is formed with a very low quantum yield. This peak was not accompanied by significant changes in the Soret absorption or the initial triplet concentration after flash excitation.

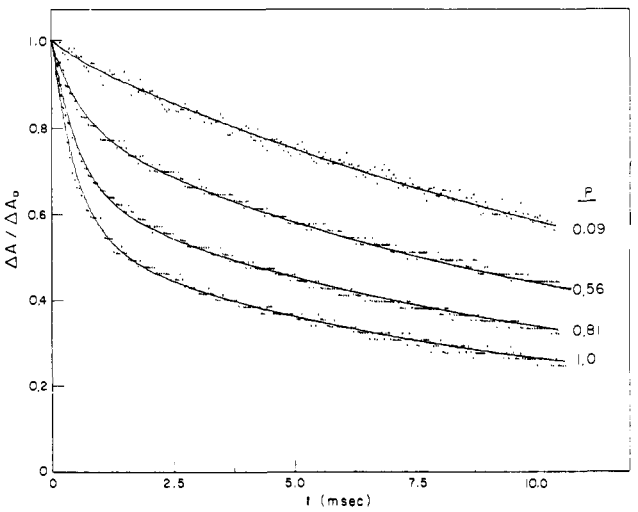

Figure 4. Decay progress curves of photoexcited ZnHb monitored at 487 nm (conditions as in Figure 1), obtained at various values for the initial fraction of excitation (P = 1.0 → 100% excitation). The theoretical curves were calculated according to the intramolecular long-range triplet–triplet energy-transfer mechanism as described in the text and embodied in eq A3.

(B) ZnHb. The decay of the ZnHb triplet in fully deoxygenated solutions differs strikingly from that of ZnMb. It was normally followed at 487 nm, where the triplet is the only absorbing species, rather than near 421 nm, where bleaching of the ground-state absorbance makes the major contribution to the observed optical transient. At very low flash intensities, resulting in excitation of only ~5% of the total ZnHb, the triplet decay is first order for more than 90% of the process, with $k_1 = 45 \pm 5$ s^{-1}. As the degree of excitation is increased, the triplet decay exhibits deviations from first-order kinetics. The latter stages of a progress curve can be fitted with a rate constant of approximately 45 s^{-1}, but the initial rate increases with flash intensity. This is dramatically shown in Figure 4, which presents curves representing the ZnHb triplet decay following 100%, 81%, 56%, and 9% excitation.

At any flash intensity (percentage of excitation) the first 5–10% of the decay curve recorded on a short time scale (0.5–1.5 ms) could be fitted very well by a linear regression to first-order kinetics giving values for the absorbance change at zero time, ΔA_0, and for the initial decay rate, k_1. The resulting rate constants were obtained over a wide range of flash intensities and are plotted in Figure 5 as a function of the corresponding value of $P = \Delta A_0/\Delta A_{max}$, with ΔA_{max} taken as the value of ΔA_0 for ~100% excitation; thus P is the fraction of zinc porphyrins excited to the triplet state. For $P \leq 0.05$, the rate constants plotted were obtained from a fit to the total progress curve, which was accurately first order, rather than from the initial rate.

Absorption changes were followed also at 421 nm, the ZnHb Soret maximum. Here the ground state absorbs approximately 5 times more than the triplet and hence one is essentially following the ground recovery. The results so obtained are qualitatively the same as at 487 nm, as demonstrated in the plot of k_1 vs. $\Delta A_0/\Delta A_{max}$ (Figure 5 (insert)), and for $P \leq 0.1$ the rate constants measured at the two wavelengths are identical, 45 s^{-1}. However, with higher excitation the k_1 obtained at 421 nm consistently were slightly lower than those observed at 487 nm. We believe that minor differences occur because the results at 421 are influenced by a transient such as that seen with ZnMb. Its existence was inferred from observations of a weak, slowly decaying transient at 434 nm, the triplet-ground state isosbestic point.

The kinetic behavior manifested in Figures 4 and 5 exhibited the following additional features. (1) Variations in the concentration of the ZnHb and in the concentration of the excited triplets, as distinguished from the fractional triplet excitation, had no effect on the kinetics. Figure 5 contains results obtained with two different samples, one containing 16 μM of ZnHb, the other 4.1

(20) Alpert, B.; Lindquist, L. *Science (Washington, D.C.)* **1974**, *187*, 836–837.
(21) Austin, R. H.; Suiling Chan, S. *Biophys. J.* **1978**, *24*, 175–182.

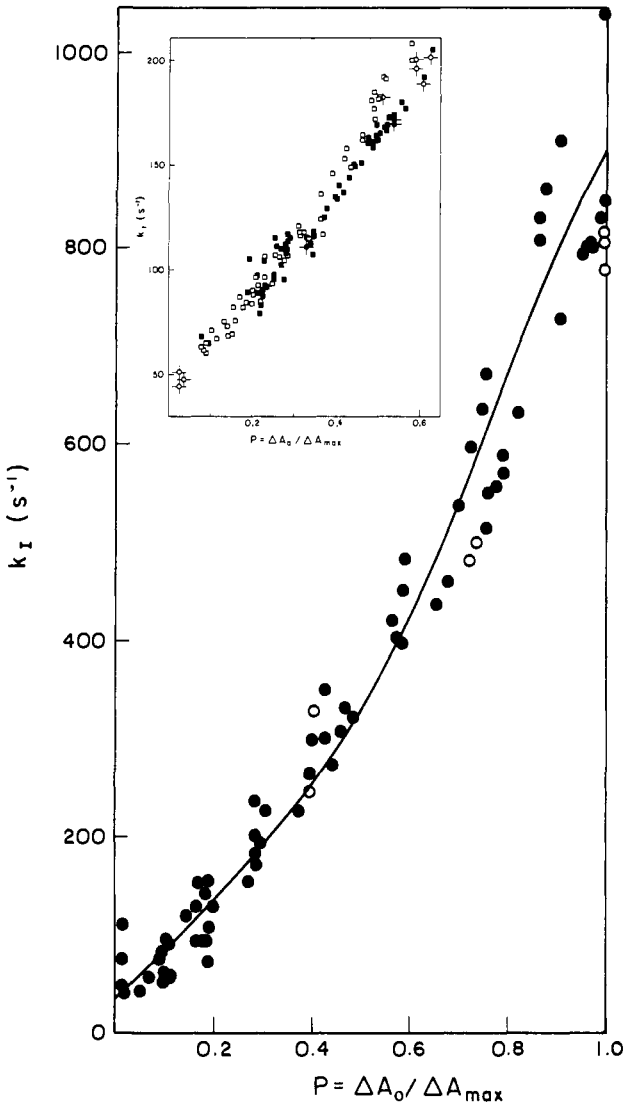

Figure 5. Dependence of the initial ZnHb triplet decay rate, k_1, on the zero-time fraction of excitation as monitored at 487 nm; (●) [ZnHb] = 13 μM in aqueous KPi buffer; (○) [ZnHb] = 13 μM in 1:1 glycerol–buffer. Insert: Dependence of the initial ZnHb triplet decay rate, k_1, on the fraction of excitation monitored at 421 nm: (□) [ZnHb] = 16 μM in aqueous buffer; (■) [ZnHb] = 4.1 μM in aqueous buffer; (◇) [NHb] = 11 μM in 1:1 glycerol–aqueous buffer; (◆) [ZnHb] = 11 μM in 1:1 glycerol–buffer at 7 °C. All other measurements are at room temperature.

μM. The dependence of k_1 on P is identical within experimental error. (2) The viscosity of the medium did not alter the results. The k_1 measured in a 1:1 mixture of glycerol and aqueous buffer were unchanged from those in the aqueous buffer. This result is observed in measurements at both 487 nm (Figure 5) and 421 nm (Figure 5, insert). (3) The temperature of the H_2O/glycerol sample was lowered from 22 to 7 °C without effect (Figure 5). (4) Changes in pH (pH 6.0–8.0) and the addition of the hemoglobin quaternary structure modifier inositol hexaphosphate also did not change the kinetic characteristics.

(III) MgMb and MgHb. The magnesium substituted proteins have been investigated primarily to provide comparisons with the zinc derivatives and as a reference for chlorophyll–protein complexes. Flash photolysis of MgMb and MgHb yields a transient difference spectra similar to the one observed with the zinc-substituted proteins, and it likewise is identified with formation of the triplet state of MgProtoPor. The triplet decay kinetics for MgMb and MgHb repeat the pattern exhibited by ZnMb and ZnHb, respectively. The MgMb triplet decay, followed at the Soret maximum, is first order with a rate constant of 24 ± 1 s^{-1} and is independent of the degree of excitation. In contrast, the

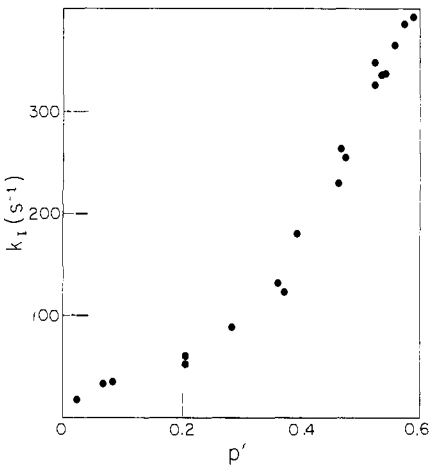

Figure 6. Dependence of the initial MgHb triplet decay rate, k_1, on the approximate fraction of excitation monitored at 480 nm in aqueous KPi buffer at ambient temperature. P' gives the degree of excitation, as defined in the text; [MgHb] ≈ 9 μM.

triplet decay in the tetrameric MgHb is like that of ZnHb, first order only at very low degrees of excitation ($k \approx 17$ s^{-1}) and deviating increasingly as a greater fraction of triplets is populated. Similarly, the initial decay rate accelerates with the increase in the degree of excitation. A plot of k_1 vs. P' is shown in Figure 6, where P' is the estimated fraction of excitation, obtained by assuming that $\Delta\epsilon$ at 480 nm is the same for MgHb and ZnHb. This assumption was needed since 100% excitation of MgHb could not be achieved.

The overall features of the zinc-substituted proteins are thus repeated with MgMb and MgHb. However, it is noteworthy that first-order decay rates for the MgPor triplet state are lower than for ZnPor; in addition, we estimate the quantum yield for MgPor triplet formation as roughly half that for ZnPor. Presumably, both differences can be explained by reduced spin–orbit coupling with the low atomic number magnesium ion.

Analysis

We now consider three mechanisms as possible explanations for the unusual ZnHb and MgHb triplet decay data: intermolecular triplet–triplet (T–T) annihilation by the short-range exchange process, chain differences within the MHb tetramer, and long-range intramolecular T–T annihilation.[22] We find that only the third is fully consistent with our results.

(I) Short-Range Intermolecular T–T Annihilation. Collisional T–T annihilation processes in aromatic compounds typically occur by electron exchange and have second-order rate constants of 10^8–10^{10} M^{-1} s^{-1}.[2] With chromophore concentrations of 16 and 4.2 μM (4 and 1.05 μM in tetrameric concentration), one might thus propose that the ZnHb and MgHb decay kinetics arise from intermolecular T–T or even triplet-ground interactions in the initial part of the decay. In particular, such contributions should increase with the degree of triplet population, as observed.

Decay processes that operate through intermolecular collisions should depend on the concentration of the colliding molecules and the diffusion coefficient, the latter being influenced by the viscosity of the medium and temperature. However, the results presented above show that the ZnHb triplet decay is completely insensitive to these factors. In addition, T–T annihilation by the exchange mechanism is accompanied by delayed fluorescence,[2] but no such emission is observed from photoexcited ZnHb or MgHb: under conditions such that normal fluorescence, decaying with the profile of the flash lamp (20 μs), was observed with a signal-to-noise ratio of over 10^3, no long-lived fluorescence could be detected.[8]

(22) Neither process 1 nor 3 of Table I need be considered. Process 1 does not result in triplet annihilation and thus cannot account for the increasing decay rate with increasing P. Process 3 is energetically unfavorable, would not be consistent with a monotonic increase of k_1 with P (Figures 5 and 6) and would give rise to delayed fluorescence, which is not observed (see below).

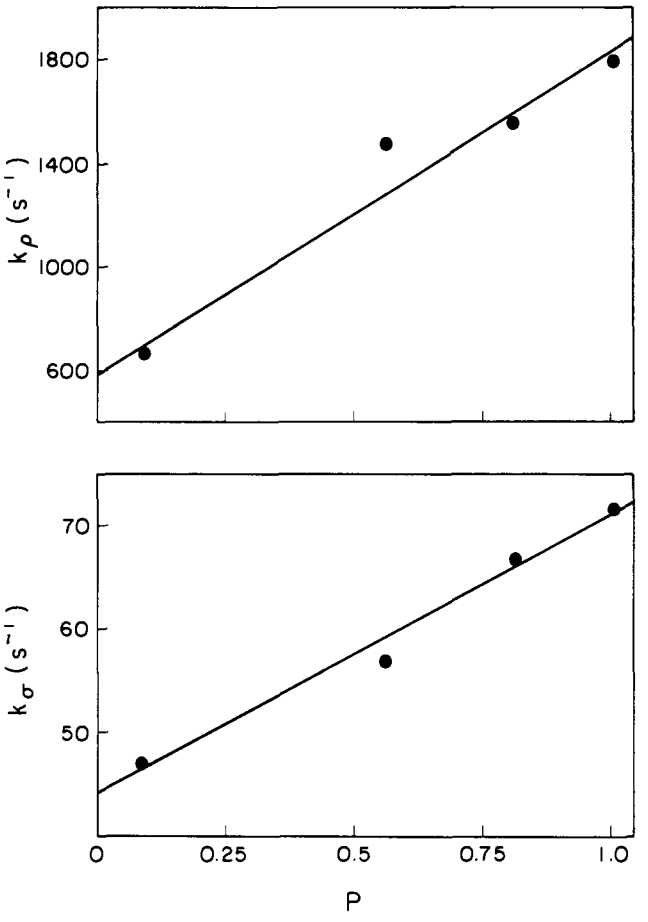

Figure 7. The results of two-exponential fits to the ZnHb triplet decay kinetics at various fractions of excitation: upper plot, dependence of the fast rate, k_ρ, on P; lower plot, dependence of the slow rate, k_σ on P.

Therefore, intermolecular self-quenching processes do not play a significant role in the decay of the ZnHb triplet state. This conclusion is further supported by the absence of second-order contributions to the decay of triplet ZnMb, since the ZnMb concentration was ~5 times higher than that of the tetrameric ZnHb.

(II) Chain Differences. Chain differences within the ZnHb tetramer could give rise to nonfirst-order decay. If a chromophore in an α chain has quantum yield and decay rate which differ from those characterizing a chromophore in a β chain, the result will be a biphasic decay described by eq 1, where ρ and σ denote the

$$\Delta A_t = \Delta A_0^\rho e^{-k_\rho t} + \Delta A_0^\sigma e^{-k_\sigma t} \quad (1)$$

rapid and slow components, respectively, and the initial absorbance will be $\Delta A_0 = \Delta A_0^\rho + \Delta A_0^\sigma$. We analyzed our fully decay curves (up to 60–80% completion) in terms of eq 1 and obtained a set of values for ΔA_0^ρ, ΔA_0^σ, k_ρ, and k_σ for each curve. The agreement between the experimental and calculated curves for any given experiment was excellent, and the dependence of $\Delta A_0^\rho/\Delta A_0$ and $\Delta A_0^\sigma/\Delta A_0$ on light intensity follows qualitatively the expected behavior for chains of unequal quantum yield. However, the values of k_ρ and k_σ were found to depend on the fraction of excitation as is shown in Figure 7. The fast rate increases roughly threefold, and the slow rate changes roughly twofold as P increases from 0 to 1. As one looks closer to $t = 0$ and follows earlier stages in the progress curve, these variations are accentuated. Such behavior is not in agreement with the model in which the two chains have different but fixed triplet decay rates. Moreover, the 10–20-fold difference in decay rates is not consistent with preliminary direct observations of triplet decay from the individual types of chains.[8] Also, the ZnPor triplet decay rates in the α and β chains, respectively, of the hybrid hemoglobins (α_2^{Zn}, β_2^{Fe}) and (α_2^{Fe}, β_2^{Zn}) are similar, and the values are in the range exhibited by ZnMb and ZnHb at low levels of excitation (P), 35–75 s^{-1}. Hence, the simple chain-difference model may be discarded.

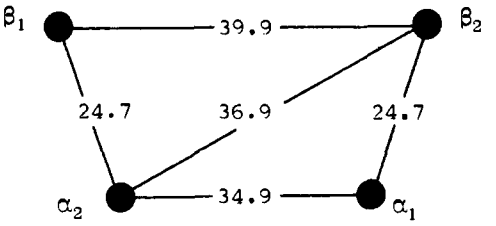

Figure 8. Metal–metal distances (Å) in a human deoxy-Hb crystal.[9]

(III) Long-Range Intramolecular Triplet–Triplet Annihilation. The only factor affecting the triplet disappearance rate is the *fraction* of excitation, P. As this fraction increases, so does the number of ZnHb tetramers with more than one excited subunit, and this is accompanied by an acceleration of the triplet decay rate. The correlation strongly suggests a mechanism of *intramolecular* T–T annihilation. Since the porphyrin moieties in the ZnHb tetramer are rigidly held 25–40 Å apart, this T–T interaction could only operate through a Förster-type energy transfer in which one excited triple-state porphyrin transfers its energy to the triplet-state porphyrin in another subunit of the *same* tetramer. The acceptor undergoes a transition to a higher excited triplet but rapidly returns to the lowest triplet by radiationless processes, and the overall result is triplet annihilation

$$T_1 + T_1 \longrightarrow T_n + S_0$$
$$T_n \xrightarrow{\text{fast}} T_1$$

This long-range annihilation process so far has been observed only once, in solid films by Kellogg.[5] However, in the MHb the requirements described by Förster for dipole–dipole radiationless energy transfer are very well satisfied. Consider the rate constant for long-range energy transfer, which may be written[23]

$$k_{D\to A} = \frac{(8.8 \times 10^{-28})K^2}{n^4 \tau R^6} \int F_D(\lambda)\epsilon_A(\lambda)\lambda^4 \, d\lambda \quad (2)$$

where K = dipole–dipole orientation factor, n = refractive index of medium, τ = natural lifetime of donor (D), and R = distance between donor and acceptor (cm). $\int F_D(\lambda)\epsilon_A(\lambda)\lambda^4 \, d\lambda$ = overlap integral (cm^6 mol^{-1}) between donor emission and acceptor absorption bands. $F_D(\lambda)$ is the normalized donor emission probability and $\epsilon_A(\lambda)$ is the molar decadic extinction spectrum of the acceptor (cm^2 mol^{-1}). First, the $T_1 \to S_0$ emission[24] and $T_1 \to T_2$ absorption bands of porphyrins[17,18] overlap considerably in the 650–850-nm region. Second, the distance between the excited centers is also well within the range of efficient energy transfer, given the long triplet-state lifetime; the intramolecular metal–metal distances in the deoxy (or T state) conformation adopted by ZnHb are shown in Figure 8.[9]

Although the metal–metal distance somewhat overestimates the appropriate value to use for the interchromophore distance, R, it is clear from Figure 8 that two porphyrin pairs, (α_1,β_2) and the symmetry-equivalent pair (α_2,β_1), are at a significantly shorter distance than any of the other three types of pairs: (α,α); (β,β); (α_1,β_1) and (α_2,β_2). One can use eq 2 to predict an approximate upper limit for k_s, the transfer rate between the close, α_1 and β_2, subunits. Using R = 25 Å, we take n = 1.4, τ = 75 ms,[24] and K^2 = 1 and assume 100% overlap between donor emission and acceptor absorption, with the latter having a triangular peak from 660 to 840 nm and ϵ_{max} (750) = 10^4 M^{-1} cm^{-1}.[18] Using these assumptions, we calculated the transfer rate to be $k_s \approx 4000$ s^{-1}; a value of roughly half this appears to be a more reasonable estimate.

The contribution of the R^6 term will decrease the other three types of transfer rates by factors of between ca. 8 and 17. The

(23) Conrad, R. H.; Brand, L. *Biochemistry* **1978**, *7*, 777–787.
(24) Gouterman, M. In "The Porphyrins"; Dolphin, D., Ed.; Academic Press: New York, 1978; Vol. III, pp 1–165.

Scheme I

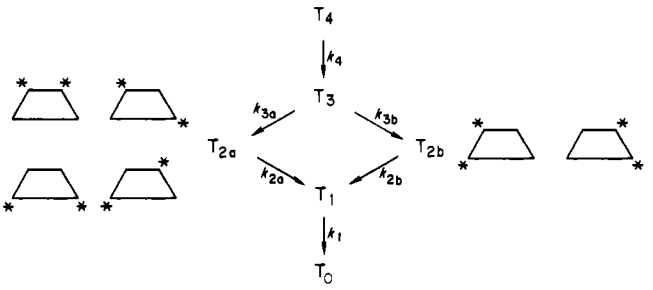

Scheme II

$$T_4 \xrightarrow{k_4} T_3 \xrightarrow{k_{3a}} T_{2a} \xrightarrow{k_{2a}} T_1 \xrightarrow{k_1} T_0$$

$$T_{2b} \xrightarrow{k_{2b}} T_1 \xrightarrow{k_1} T_0$$

relative orientations of the porphyrin planes within the various pairs will also affect the transfer rates through the term K_2[25] but to a much lesser extent because of the degenerate character of the metalloporphyrin excited states.

These considerations permit us to quantitatively interpret the triplet decay kinetics of the tetrameric MHb through a scheme based on the occurrence of long-range, intramolecular T–T annihilation. To begin, by symmetry the two pairs of chains (α_1,β_2) and (α_2,β_1) will exhibit the same, high, T–T annihilation rate constant, which we label as k_s. There are four pairs of chains with much slower rates, (β,β), (α,α), (α_1,β_1), and (α_2,β_2); as a first approximation, we assign a single rate constant, k_L, to these four energy-transfer processes. Each triplet can also decay unimolecularly with a rate constant k_m which we assume to be the same for both subunits. Equation 3 summarizes these intratetramer decay processes.

$$T_1 \xrightarrow{k_m} S_0 \tag{3}$$

$$T_1 + T_1 \xrightarrow{k_L \text{ or } k_s} T_1 + S_0$$

The complete decay of a fully excited tetramer is described by Scheme I, in which an asterisk denotes a subunit with an excited chromophore, where T_4 represents a tetramer with four excited triplets and T_3, all arrangements with three excitations on a tetramer. The symbol T_{2a} represents the set of tetramers having two excitations arranged so that they can annihilate only with the slow rate, k_L; T_{2b} denotes the two arrangements of two excitations which have the high annihilation rate, k_s. Consideration of all the individual processes subsumed in Scheme I gives the rate constants $k_{i\gamma}$ as functions of k_m, k_L, and k_s.

$$k_4 = 4k_m + 4k_L + 2k_s \tag{4}$$

$$k_{3a} = 2k_m + k_L + k_s$$

$$k_{3b} = k_m + k_L$$

$$k_{2a} = 2k_m + k_L$$

$$k_{2b} = 2k_m + k_s$$

$$k_1 = k_m$$

Since $k_s \gg k_L$ and k_m and hence $k_{3a} \gg k_{3b}$, then the path from T_3 to T_{2b} will contribute negligibly to the decay of T_3. However, when triplet excitation is less than 100%, finite concentrations of T_{2b} will be initially created during the flash, and so the decay process k_{2b} must be retained in general. Thus, for an arbitrary degree of excitation the kinetic model simplifies further into two independent reactions (Scheme II).

The integrated rate equations for this scheme are[26]

$$[T_4]_t = [T_4]_0 e^{-k_4 t} \tag{5}$$

$$[T_3]_t = \frac{-k_4}{(k_4 - k_{3a})}[T_4]_0 e^{-k_4 t} + \left[\frac{k_4}{(k_4 - k_{3a})}[T_4]_0 + [T_3]_0\right] e^{-k_{3a} t}$$

$$[T_{2a}]_t = \frac{k_4 k_{3a}}{(k_4 - k_{3a})(k_4 - k_{2a})}[T_4]_0 e^{-k_4 t} - \left[\frac{k_{3a} k_4}{(k_4 - k_{3a})(k_{3a} - k_{2a})}[T_4]_0 + \frac{k_{3a}}{(k_{3a} - k_{2a})}[T_3]_0\right] e^{-k_{3a} t} + \left[\frac{k_4 k_{3a}}{(k_4 - k_{2a})(k_{3a} - k_{2a})}[T_4]_0 + \frac{k_{3a}}{(k_{3a} - k_{2a})}[T_3]_0 + [T_{2a}]_0\right] e^{-k_{2a} t}$$

$$[T_{2b}]_t = [T_{2b}]_0 e^{-k_{2b} t}$$

$$[T_1]_t = -\frac{k_4 k_{3a} k_{2a}}{(k_4 - k_{3a})(k_4 - k_{2a})(k_4 - k_1)}[T_4]_0 e^{-k_4 t} + \left[\frac{k_4 k_{3a} k_{2a}}{(k_4 - k_{3a})(k_{3a} - k_{2a})(k_{3a} - k_1)}[T_4]_0 + \frac{k_{3a} k_{2a}}{(k_{3a} - k_{2a})(k_{3a} - k_1)}[T_3]_0\right] e^{-k_{3a} t} - \left[\frac{k_4 k_{3a} k_{2a}}{(k_4 - k_{2a})(k_{3a} - k_{2a})(k_{2a} - k_1)}[T_4]_0 + \frac{k_{3a} k_{2a}}{(k_{3a} - k_{2a})(k_{2a} - k_1)}[T_3]_0 + \frac{k_{2a}}{(k_{2a} - k_1)}[T_{2a}]_0\right] e^{-k_{2a} t} + \left[\frac{k_1 k_{3a} k_{2a}}{(k_4 - k_1)(k_{3a} - k_1)(k_{2a} - k_1)}[T_4]_0 + \frac{k_{3a} k_{2a}}{(k_{3a} - k_1)(k_{2a} - k_1)}[T_3]_0 + \frac{k_{2a}}{(k_{2a} - k_1)}[T_{2a}]_0 + [T_1]_0\right] e^{-k_1 t} + \frac{k_{2b}}{k_{2b} - k_1}[T_{2b}]_0 (e^{-k_1 t} - e^{-k_{2b} t})$$

$$[T_0]_t = [T] - \sum_{i \neq 0} \sum_{\gamma} [T_{i\gamma}]_t$$

$[T]$ is the total tetramer concentration, $[T_{i\gamma}]_t$ is the total concentration at time t of the γ class of tetramers with i triplet chromophores, and $[T_{i\gamma}]_0$ is the concentration immediately after the flash ($t = 0$); in Scheme II, only for $i = 2$ is the consideration of two different classes, λ = a and b required.

The absorption change at a time t after flash excitation is given by eq 6, where $\Delta\epsilon$ is the extinction coefficient on a monomer basis

$$\Delta A_t = \Delta\epsilon l \sum_{i=1}^{4} \sum_{\gamma} i[T_{i\gamma}]_t \tag{6}$$

and l the path length. In the Appendix we extend this equation to obtain an expression for ΔA_t within Scheme II assuming an arbitrary degree of excitation and also allowing for differing triplet quantum yields in α and β subunits. In this case P is an average of possibly differing subunit excitation probabilities, P_1 and P_2. These in turn are related through r, the ratio of quantum yields, ϕ_i, for the individual chains, $0 \leq r = \phi_2/\phi_1 \leq 1$. For a given light intensity, $P_1 = P_2$ and P when $r = 1$ and the ratio P_2/P_1 decreases monotonically with r. We further derive an equation for the triplet decay immediately following flash excitation of arbitrary strength, when $k_{i\gamma} \ll 1$ for all $k_{i\gamma}$

$$\Delta A_t \underset{k_{i\gamma} t \ll 1}{\rightarrow} \Delta A_0 (1 - k_1 t) \tag{A9}$$

(25) Dale, R. E.; Eisinger, J. *Biopolymers* **1974**, *13*, 1573–1605.

(26) Rodiguin, N. M.; Rodiguina, E. N. "Consecutive Chemical Reactions"; Van Nostrand, Princeton, N.J., 1964.

The initial decay rate, k_1, is dependent on P_1 and P_2 and thus, through eq A7 and A8, on the value of r and the measured average excitation P. The general form of k_I is given in the Appendix, eq A10; the explicit result for Scheme II is

$$k_1 = \left(\frac{P_1^2P_2^2}{P} - P_1P_2 + 1\right)k_m + \left(\frac{P_1^2P_2^2}{P} - P_1P_2 + P\right)k_L + \frac{P_1P_2}{2P}k_s \quad (7)$$

Equations A9 and A3 respectively provide kinetic expressions for short-time and overall triplet decay curves based on Scheme II for long-range triplet–triplet annihilation within a ZnHb tetramer. We have used the two approaches jointly in order to extract the triplet–triplet energy-transfer rate constants.

Considering the short-time results, eq 7 can be rearranged to give the form

$$\frac{k_1 - (V+1)k_m}{(V+P)} = k_L + \frac{P_1P_2}{2P(V+P)}k_S \quad (8)$$

where $V = P_1^2P_2^2/P - P_1P_2$. Equation 8 can be schematically rewritten in terms of coefficients calculable from k_1 and P, once values for k_m and r are fixed.

$$A(k_1, P, k_m, r) = k_L + B(P,r)k_s \quad (9)$$

Since the overall decay rate should approach k_m as $P \rightarrow 0$, an initial guess of $k_m \approx 45$ cm^{-1} s^{-1} was employed, although considerations presented below led to the use of a range of values, 25 s$^{-1} \leq k_m \leq 45$ s^{-1}. The values of k_L and k_s are then derivable from a linear fit of eq 8 to the initial-rate data (Figure 5), providing a value of r is adopted for use in eq A8. For each value of r, one obtains a set of k_L and k_s values. We have examined the range $0.1 \leq r \leq 1.0$ and find that the shape of the k_1 vs. P curve is extremely sensitive to r, becoming too flat or too curved when r is outside the range 0.16 ± 0.03. In addition, for appreciably different values of r, k_L becomes negative and large. When $r = 0.16 \pm 0.03$ and $k_m = 35 \pm 10$ s^{-1}, the regression results for the T–T annihilation rate constants are $k_L = 50 \pm 40$ s^{-1} and $k_s = 1600 \pm 200$ s^{-1}. When substituted into eq 7, these values accurately reproduce the data of Figure 5.

Although the value of r is quite well specified by analysis of the initial-rate data, the rate constants obtained through this treatment only provide good first approximations to the proper values. First, it is straightforward to show that the least-squares derivation of k_L and k_s, using eq 9 and a set of (k_1, P) obtained by varying the flash intensity, is not a statistically rigorous procedure. More immediately, while keeping r fixed, we calculated k_1 vs. P curves for a variety of k_L, k_s pairs in the neighborhood of the above values and found that adequate fits were possible over a range of rates.

In contrast, the full decay curves are extremely sensitive to the precise values of the rate constants. Thus, the full decay curves such as those of Figure 4 were employed to obtain final values of k_L, k_s, and k_m. With r fixed at 0.16, k_L, k_s, and k_m were varied until a satisfactory agreement was obtained between the calculated progress curves and the traces observed with varying degrees of excitation (P). The technique used was to successively examine curves with increasing P and thus with increasing contributions from tetramers with more than one triplet. Figure 9 presents progress curves for three different fractions of excitation; in each case the individual T_i are calculated from eq 5 with the final rate constants. At very low excitation, (Figure 9, $P = 0.09$), one essentially observes only the decay of T_1; the T_i with $i > 1$ contribute only at short time and even then almost negligibly. As the fraction of excited triplets increases and T_2 becomes populated (Figure 9, $P = 0.56$), k_L increasingly influences the decay curve through k_{2a} (eq 4), but k_s contributes very little through k_{2b} and only at the initial part of the decay; k_L was determined from such curves. With k_m and k_L fixed, the value of k_s was obtained from data with high levels of excitation (Figure 9, $P = 1$) in which case the rapidly decaying species T_4 and T_3 make a major contribution to the overall progress curve through the processes involving k_s.

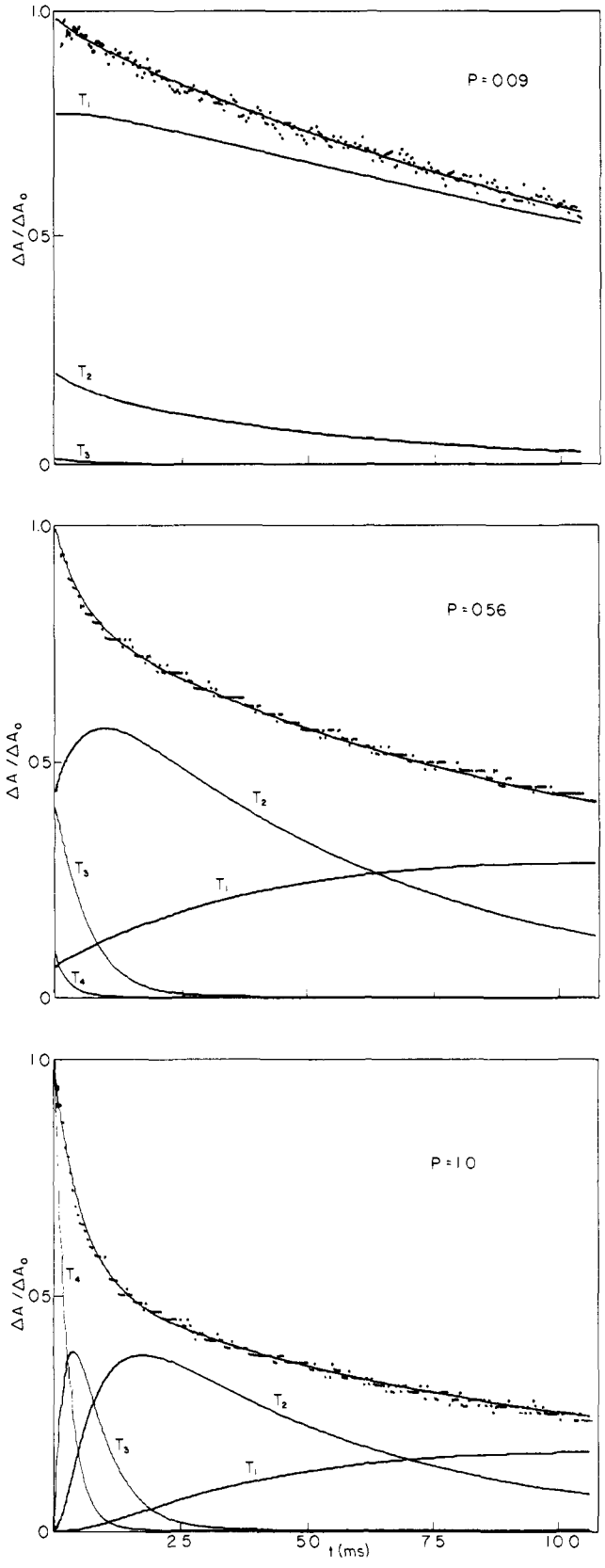

Figure 9. The experimental and best-fit theoretical progress curves for ZnHb triplet decay at various fractions of excitation. Included are the contributions from tetramers, T_i, with $i = 1, 2, 3$, and 4 excited triplets. The concentrations of excited species and their decay curves were calculated from eq 5 by using the final values of k_s, k_L, and k_m as described in the text.

The optimal theoretical curves obtained from the equations based on Scheme II are shown in Figure 4. They employ the final

best estimates for the ZnHb triplet-decay rate constants: k_s = 1550 s^{-1}, k_L = 100 ± 15 s^{-1}, and k_m = 42 ± 5 s^{-1}. A single value of k_s could be used to reproduce the progress curves at all values of P. The error figures for k_L and k_m reflect the fact that fitting all four decay traces required such an additional minor variation in these rates. For example, while the 100% excitation curve was best fitted with k_L = 115 s^{-1}, the lower excitation curves were fitted with k_L = 85 s^{-1}; the lowest light intensity data (Figure 4, P = 0.09) was fitted with k_m = 47 s^{-1} while the other three traces in Figure 4, with k_m = 37 s^{-1}. These small but real variations in k_m and k_L will be further examined in the discussion.

A theoretical k_1 vs. P curve calculated from eq 7 by using the final k_s and the average values for k_L and k_m is shown in Figure 5. It is clear that the experimental data and the theoretical curves are in excellent agreement for both the initial conditions (Figure 5) and the overall decay (Figure 4).

Discussion

The only previous report of long-range energy transfer between photoexcited triplet states was that of Kellogg.[5] He detected the phenomenon in solid cellulose acetate films by observing a concentration dependent quenching of phenanthrene phosphorescence unaccompanied by delayed fluorescence. We have now observed the same energy-transfer process in fluid solution, occurring intramolecularly between pairs of excited-triplet metallomacrocycles within the MHb tetramer. We are able to observe this process because incorporation of the chromophore into a protein complex effectively eliminates the collisional triplet self-quenching process. Thus, relatively high concentrations of the monomeric ZnMb and MgMb exhibit first-order triplet decay with no evidence for a second-order contribution. In contrast, the triplet decay kinetics of solution metalloporphyrins at comparable concentrations is usually dominated by the bimolecular exchange process.[17]

The study of triplet energy transfer within the tetrameric MHb unit has provided us with an opportunity unmatched in any other study of long-range Förster-type transfer; we have been able to directly obtain the energy-transfer rate constants for pairs of chromophores held fixed at known distances and orientations. The excellent agreement between the experimental data and the simulated curves (Figures 4 and 5) indicates the overall validity of the simplified decay Scheme II. The resulting k_s, representing the α_1–β_2 transfer process, is in excellent accord with the rate estimated from eq 2. The value of k_L represents an average of the three different slow rates and as such is also in satisfactory agreement with expectation.

A somewhat surprising result is the noticeable chain difference in triplet-state quantum yields required by the ZnHb initial rate data. Since this is not believed to result from differences in optical absorption spectra,[8] it appears to indicate an appreciable influence of the protein environment on excited-state photophysical processes. As such, it may relate to apparent differences among photodissociation quantum yields of carbonylferroporphyrins in Mb and in Hb in its various conformations.[27,28]

The experimental values of k_s, k_L, and k_m directly justify neglect of the pathway $T_3 \rightarrow T_{2b}$ in Scheme II. Since $k_{3a}/k_{3b} \approx 12$, over 90% of T_3 decays via the $T_3 \rightarrow T_{2a}$ path. This graphically illustrates how specific arrangements of chlorophylls in a protein matrix might create preferred pathways for energy migration. In addition, it is possible that there are circumstances under which the specific long-range annihilation process studied here might act to limit the efficiency of photosynthesis.

The simplifications incorporated in Scheme II are not totally without consequence. In particular, the assignment of a single rate constant k_L to the three different slow T–T annihilation processes and of a single k_m to the unimolecular decay in both chains leads to a small but real variation of the apparent k_L and k_m with excitation level, P. At low P, the decays are fitted with k_L = 85 and k_m = 47 s^{-1} and at high P with k_L = 115 s^{-1} and k_m = 37 s^{-1}. The detection of such a small rate variation is possible because of the appreciable chain differences in triplet quantum yields. When $P \ll 1$, the triplets of one chain type are populated preferentially, and thus transfer between like chains, either α–α or β–β, dominates k_L. As $P \rightarrow 1$ all four slow transfers ($\alpha\alpha$, $\beta\beta$, $\alpha^1\beta_1$, and $\alpha_2\beta_2$) contribute. In a similar manner, at low P, k_m is essentially that of the high quantum yield chain, but as $P \rightarrow 1$ it is a composite.

Despite the minor limitations of Scheme II we have chosen not to attempt to fit the decay kinetics with more general expressions. In part this is because an attempt to evaluate several small and similar rate constants from the present data probably would not be meaningful. More important, we have begun a variety of experiments with isolated chains and with mixed-metal hybrid hemoglobin, both at room temperature by transient absorption and at low temperatures by emission, which will give more direct determinations of some of these rate processes. Measurements on chlorophyll-substituted hemoglobin[29] are also in progress. We further anticipate that extensions of the quenching experiments will permit observation of photochemical as well as photophysical processes involving a metallomacrocycle–protein complex.

Acknowledgment. We gratefully thank Professor E. Zemel for discussions regrading the statistical analysis of MHb decay kinetics and Professor K. G. Spears and Mr. S. Brugge for assistance in installing the laser. This work was supported by grants from the NSF (No. PCM 7681304) and NIH (No. HL 13531).

Appendix

Flash excitation produces at time zero a distribution of tetramers with from i = 0 to i = 4 chromophores in their lowest triplet state. The $[T_{i\gamma}]_0$ of eq 5 can further be written as eq A1, where $f_{i\gamma}$ is

$$[T_{i\gamma}]_0 = f_{i\gamma}[T] \tag{A1}$$

the fraction of tetramers of the class $T_{i\gamma}$ which has been created during the flash and [T] is the total concentration of tetramers. The $[T_{i\gamma}]_t$ can be rewritten as eq A2, where the $[T_{i\gamma}']_t$ is given

$$[T_{i\gamma}]_t = [T][T_{i\gamma}']_t \tag{A2}$$

by equations identical with eq 5 except that all $[T_{i\gamma}]_0$ are replaced by $f_{i\gamma}$. In terms of the $[T_{i\gamma}']_t$, the absorption changes at any time following flash excitation, eq 6, now becomes eq A3, where $\Delta A_{max} = 4\Delta\epsilon l[T]$.

$$\Delta A_t = \frac{\Delta A_{max}}{4} \sum_{i=1}^{4} \sum_{\gamma} i[T_{i\gamma}']_t \tag{A3}$$

The $f_{i\gamma}$ can be calculated from the overall probability of finding a subunit in the excited triplet state, $P = \Delta A_0/\Delta A_{max}$. Allowing for the possibility that the α and β chains have different quantum yields, we define P_1 and P_2 as the excitation probabilities of the porphyrins in the two types of subunits, without implication as to which corresponds to α and which to β. In this case the measured probability P is an average of the individual quantities

$$P = (P_1 + P_2)/2 \tag{A4}$$

The fraction of tetramers with a given excitation pattern is

$$f_i^{j,k} = f_{(j+k)} = \frac{2!}{j!(2-j)!} P_1^j(1-P_1)^{(2-j)} \frac{2!}{k!(2-k)!} P_2^k(1-P_2)^{(2-k)} \tag{A5}$$

where j and k represent the number of excitations on each of the two different subunits, j and k = 0, 1, and 2 and $i = j + k$. In the case of i = 2 the values of j and k as well as the identity of the pair of excited subunits determine whether the tetramer falls into class T_{2a} or T_{2b}.

The values of P_1 and P_2 for a given measured P are obtained as follows: the probability of exciting a chromophore in a type

(27) Hoffman, B. M.; Gibson, Q. N. *Proc. Natl. Acad. Sci. U.S.A.* **1978**, *75*, 21–25.
(28) Brunori, M.; Giacometti, G. M.; Antonini, E.; Wyman, J. *Proc. Natl. Acad. Sci. U.S.A.* **1973**, *70*, 3141–3144.
(29) (a) Davis, R. C.; Pearlstein, R. M. *Nature (London)* **1979**, *280*, 413–415. (b) Boxer, S. G.; Wright, K. A. *J. Am. Chem. Soc.* **1979**, *79*, 6791–6794.

η chain by a flash of intensity I is related to the quantum yield (ϕ_η) by the expression[27]

$$-\ln (1 - P_\eta) \equiv -\ln (\bar{P}_\eta) \propto \phi_\eta I \quad \text{(A6)}$$

Letting the quantum yields for triplet formation in the two subunits be ϕ_1 and $\phi_2 = r\phi_1$ ($0 \leq r \leq 1$), it follows that

$$\bar{P}_2 = \bar{P}_1 r \quad \text{(A7)}$$

Substituting this relation into eq A4, one obtains an implicit formula for calculating $\bar{P}_1$ and consequently P_1 and P_2, given the average excitation level, P, and $\bar{P} = 1 - P$ and an assumed value of r.

$$\bar{P}_1 = \frac{2\bar{P}}{1 + \bar{P}_1^{(r-1)}} \quad \text{(A8)}$$

The value of r is unknown in advance but can be estimated rather well from the initial rate data as is described in the text.

Under initial conditions, namely $k_{i\gamma}t \ll 1$ for all i, eq A3 reduces to a linear form

$$\Delta A_t = \Delta A_0(1 - k_1 t) \quad \text{(A9)}$$

where

$$k_1 = \frac{\sum_{i=1}^{4}\sum_{\gamma} k_{i\gamma} f_{i\gamma}}{\sum_{i=1}^{4}\sum_{\gamma} f_{i\gamma} i} \quad \text{(A10)}$$

The $k_{i\gamma}$ are given in eq 4 and the $f_{i\gamma}$ are defined in terms of the f_l^{jk} of eq A5.

General-Acid Catalysis of Imidazolidine Ring Opening. The Hydrolysis of Ethyl *N,N'*-[1-(*p*-(Dimethylamino)phenyl)propenediyl]-*p*-[((2-tetrahydroquinolinyl)methylene)amino]benzoate

Thomas H. Fife* and August M. Pellino

Contribution from the Department of Biochemistry, University of Southern California, Los Angeles, California. *Received June 30, 1980*

Abstract: Ring opening of ethyl *N,N'*-[1-(*p*-(dimethylamino)phenyl)propenediyl]-*p*-[((2-tetrahydroquinolinyl)methylene)-amino]benzoate in 50% dioxane–H_2O at 30 °C proceeds with formation of a Schiff base having λ_{max} = 539 nm. This Schiff base is that formed by breaking of the C–N(10) bond as indicated by the spectral data; i.e., the most stable Schiff base is formed with expulsion of the nitrogen of lowest pK_a. Ring opening is catalyzed by hydronium ion with the second-order rate constant $k_H = 1.4 \times 10^5$ M^{-1} s^{-1}. The Schiff base intermediate is not detectable at pH values greater than 7, being present only at low steady-state concentrations (pK_{eq} for ring opening is 4.8). Hydrolysis of the Schiff base proceeds 10^5–10^6-fold more slowly than ring opening. Hydronium ion catalysis occurs at low pH with $k_H = 0.13$ M^{-1} s^{-1}. General-acid catalysis by a series of buffer acids was found in ring opening with a Brønsted α coefficient of 0.7. Thus, protonation of nitrogen and C–N bond breaking take place in a concerted manner with proton transfer well advanced in the transition state. General-acid catalysis only occurs in reactions of the neutral species. Addition of a proton to give a monocationic species abolishes general-acid catalysis in ring opening, although the second-order rate constant for hydronium ion catalysis is only reduced sixfold. Thus, carbonium ion stabilization and leaving group effects are much more important in giving rise to general-acid catalysis than basicity considerations. The α of 0.7 for the imidazolidine is higher than that obtained in ring opening of 2-(*p*-(dimethyl-amino)styryl)-*N*-phenyl-1,3-oxazolidine (0.5), which primarily reflects the effect on α of the basicity of the leaving groups (*p*-carbethoxyphenyl-substituted nitrogen vs. oxygen). The α in imidazolidine ring opening is identical with that for hydrolysis of 2-(*p*-(dimethylamino)styryl)-1,3-dioxolane (0.7), which indicates that carbonium ion stabilization, leaving group ability, and basicity factors are compensating in the two reactions in regard to the effect on α. Although basicity of the nitrogens of the imidazolidine ring is very high in comparison with the analogous acetal, general-acid catalysis still occurs because bond breaking is facile, and the same factors are important in the two reactions.

The important enzyme cofactor N^5,N^{10}-methylenetetrahydrofolic acid contains an imidazolidine ring which undergoes ring opening during its enzyme mediated reactions.[1] This ring opening may occur with general-acid catalysis by functional groups in the active sites of the enzymes as has been suggested for thymidylate synthetase.[2] Thus, an understanding of the chemistry of imidazolidine ring opening is of critical importance to understanding the mechanism of action of the cofactor. It is also of great theoretical importance to determine the factors that might facilitate general-acid catalysis in reactions of compounds of relatively high basicity.[3,4]

A Schiff base has been observed spectroscopically in ring opening of 2-(substituted benzaldehyde)-1,3-imidazolidines[5,6] at pH <5, but searches for general-acid catalysis were made difficult by the fact that a Schiff base could not be observed at pH >5, only low steady-state concentrations being present in the hydrolysis reactions. Thus, the effect of weak acids, which offer the best chance for success,[7] could not be studied. Ring opening of *N*-alkylimidazolidines of *p*-(dimethylamino)cinnamaldehyde can be

(1) Rader, J. I.; Huennekens, F. M. In "The Enzymes", 3rd ed.; Boyer, P. D., Ed.; Academic Press: New York, 1973; Vol. 9.
(2) Benkovic, S. J.; Bullard, W. P. *Prog. Bioorg. Chem.* **1973**, *2*, 133.
(3) Fife, T. H.; Pellino, A. M. *J. Am. Chem. Soc.* **1980**, *102*, 3062.
(4) Jencks, W. P. *Chem. Rev.* **1972**, *72*, 705.
(5) Fife, T. H.; Hutchins, J. E. C. *J. Am. Chem. Soc.* **1976**, *98*, 2536.
(6) Fife, T. H.; Hutchins, J. E. C.; Pellino, A. M. *J. Am. Chem. Soc.* **1978**, *100*, 6455.
(7) Fife, T. H.; Anderson, E. *J. Org. Chem.* **1971**, *36*, 2357.

0002-7863/81/1503-1201$01.25/0